Examination of the local structure in composite and low dimension semiconductor by X-ray Absorption Spectroscopy

K. Lawniczak-Jablonska*, I.N. Demchenko , E. Piskorska, A. Wolska, E. Talik, [1] D.N. Zakharov,[2] and Z. Liliental-Weber[2]

 Institute of Physics Polish Academy of Science, Al. Lotników 32/46, 02-668 Warsaw, Poland

[1] Institute of Physics, University of Silesia, ul. Uniwersytecka 4, 40-007 Katowice, Poland

[2]Lawrence Berkeley National Laboratory, m/s 62R203-8255, Berkeley, CA 94720, USA

Abstract

X-ray absorption methods have been successfully used to obtain quantitative information about local atomic composition of two different materials. X-ray Absorption Near Edge Structure analysis and X-Ray Photoelectron Spectroscopy allowed us to determine seven chemical compounds and their concentrations in c-BN composite. Use of Extended X-ray Absorption Fine Structure in combination with Transmission Electron Microscopy enabled us to determine the composition and size of buried Ge quantum dots. It was found that the quantum dots consisted out of pure Ge core covered by 1-2 monolayers of a layer rich in Si.

*Corresponding author: jablo@ifpan.edu.pl

1. Introduction

Synchrotron radiation sources with very high intensity radiation in a broad range of energy, and with linear or circular polarization, have lead to the rapid development of X-ray Absorption Spectroscopy (XAS). The advanced analysis of X-ray Absorption Near Edge Structure (XANES) and Extended X-ray Absorption Fine Structure (EXAFS) spectra offers a unique possibility for examining local structure. The most important feature of the x-ray absorption spectroscopy is the elemental sensitivity that allows us to separate structural information concerning a particular element in a multi-element compound even if the content of this element is very low and the system is disordered.

The shape of the XANES spectra depends on the density of the unoccupied states in a given compound, and thus it can be considered as fingerprint of chemical bonds. The absorption edge energy can be correlated with charge transfer in the investigated element [1, 2]. In the case when a mixture of the several compounds containing the same element is present in the investigated sample, the analyzed spectrum is a weighted sum of the single-phase spectra of these compounds. This can be used for quantitative estimation of the concentration of particular phases in a sample [3]. Here this method was applied to determine the composition of disordered composites based on cubic boron nitride (c-BN), as well as a composition of Ge quantum dots buried in Si matrix.

The EXAFS oscillations are created in X-ray absorption process due to the scattering of internal photoelectrons on the neighboring atoms, therefore, the analysis of these oscillations is a source of information on a short-range order in the samples. This is of particular value in the case of investigation of buried low dimensional structures or dopants in the semiconductors. The example of application of this technique to study strain and Si concentration inside Ge quantum dots formed in silicon is presented in correlation with the Transmission Electron Microscopy (TEM) results.

The BN composites are attractive for industry due their super-hardness, combined high hardness and low friction, high corrosion resistance, attractive thermal and electrical properties [4]. In order to understand the origin of these exceptional properties, it is necessary to understand the multiphase composition and microstructure of these materials. During technological process of composite preparation the formation of several phases takes place. To optimize the properties of composites it is important not only to detect the existence of a particular phase but also to determine its concentration. The coexistence of many phases with low concentration and the high hardness of the material create difficulties for quantitative X-Ray Diffraction (XRD) phase analysis [5]. Therefore, the quantitative phase analysis was performed using the XANES analysis and X-Ray Photoelectron Spectroscopy (XPS).

Semiconductor nanostructures are the objects of great attention of scientists in the last decades due to theirs many unique properties. At present the principal direction of technical application of self-assembled quantum dots (QDs) is in development of semi-conducting lasers for fiber-optic connection lines and optical recording. Therefore, many efforts are directed on growth of optically active QDs (the region ~1.3 - ~1.7 μm), increase homogeneity both in terms of concentration and surface density, and also decrease defect concentration inside the QDs.

In spite of very active studies of the properties of Si/Ge/Si structures and Si/Ge superlattices applying different methods, there are still some questions concerning understanding and controlling the quantum dot composition in buried layers. The estimation of the core composition of Ge QDs and the thickness and composition of the subsurface layer of the dots is not an easy task. Due to the problem related to the exposure to the air this information can be obtained only by surface techniques applied for in-situ grown structures. Covering the QDs by a Si cap can introduce an additional stress. It will be shown that x-ray absorption spectroscopy is a perfect tool for estimating the average concentration of a

particular element inside the QDs and for determining the thickness and composition of the subsurface layer surrounding each dot.

2. Experiment

2.1 Samples preparation

The composite sample was prepared from the mixture in ethyl alcohol of cubic boron nitride powder (ABN- 300, De Beers, 3-5μm grains size) with titanium silicon carbide powder (Ti$_3$SiC$_2$) taken with 1:3 volume ratio. Then the powder was pressed into pellet of 14 mm diameter under 10^9 Pa and temperature of 1750^0 C for 3 minutes. These conditions are typical for the technology of c-BN base composites. Commercial powders of TiB$_2$, TiC (HC Starck) and TiSi$_2$, TiO$_2$, TiC$_{0.3}$N$_{0.7}$, TiC$_{0.7}$N$_{0.3}$, Ti$_3$SiC$_2$, Si$_3$N$_4$, SiC, SiO$_2$, c-BN with 3-5μm grain sizes were used as reference samples.

The samples with Ge layer buried in silicon matrix were grown by MBE on Si(001) substrates. A homoepitaxial Si buffer layer with the thickness of 100 nm was grown at Si substrate temperature 600^{0}C. In order to reduce the size of QDs, the temperature of Si buffer was decreased to 210^{0}C and a layer of germanium with a nominal thickness of 7 and 12 monolayers (ML) was grown and subsequently capped by a 20 nm thick Si layer at 430^{0}C. The detailed description of the growth procedure was presented earlier [6, 7].

The set of Ge$_x$Si$_{1-x}$ alloys reference samples was also grown by MBE on Si(001) substrate with the thickness close to 1 μm with different content of Ge – Ge$_{1.0}$Si$_{0.0}$, Ge$_{0.5}$Si$_{0.5}$, Ge$_{0.1}$Si$_{0.9}$. In-situ reflection high-energy electron diffraction (RHEED) showed spotty patterns confirming formation of Ge dots. Si/Ge/Si(001) samples with the nominal thickness of 7 and 12ML of Ge were also investigated by cross-section Transmission Electron Microscopy (TEM). The (110) cross-section specimens for High Resolution Electron Microscopy (HREM) were prepared by mechanical polishing and a standard Ar ion milling using low voltage and low ion-beam angle in order to avoid the damage of the sample.

2.2 Measurement techniques

The XANES spectra at the K-edge of all elements present in BN-base composites were measured for all single-phase reference samples. The studies were performed at Advanced Light Source (ALS, beamline 6. 3. 1) in Lawrence Berkeley National Laboratory (LBNL, Berkeley, USA). All samples were electrically isolated from the spectrometer and the drain current from the samples was measured (total electron yield mode).

The EXAFS spectra from a sample with a nominal 12 ML thick Ge layer were recorded at the room temperature using the double crystal Si(111) monochromator at the A1 station in HASYLAB, Hamburg, Germany. The sample with a nominal 7 ML thick Ge layer was measured at liquid nitrogen temperature. The experiments were performed at the K-edge of Ge (11103 eV) using seven-element Si fluorescence detector. The spectra were measured at the angle of 45^0 between the sample surface and the polarization vector of the synchrotron radiation. The reference Ge_xSi_{1-x} alloys were measured using the drain current method at the normal incidence angle.

The Atoms, Athena and Artemis programs , based on IFEFFIT data analysis package, were applied to data processing. The theoretical amplitudes and phases were calculated by FEFF8. The same data analyzing procedure was applied to all data to keep the systematic error at the same level. The amplitude-dumping factor S_0^2 equal to 0.91 was determined by fitting data for germanium crystal. The threshold energy was deduced as a maximum of the first derivative of each EXAFS spectrum. The oscillations function $\chi(k)$ for each sample was multiplied by a square of the photoelectron wave vector modulus, k^2. The Fourier transformation was computed using the Hanning filtering function. The inset limits for photoelectron wave vector for the Fourier Transform (FT) were from 3.80 to 12.28 $Å^{-1}$.

HREM experiments of investigated samples were carried out at the room temperature using JEOL 3010 microscope operating at 300 keV (point-to-point resolution of 2.1 Å).

The X-ray photoelectron spectra of composites were recorded with the Perkin-Elmer 5400 small-spot ESCA spectrometer equipped with a hemispherical analyzer at the University in Turku, Finland. The binding energy of the $TiC_{0.3}N_{0.7}$, $TiC_{0.7}N_{0.3}$ and Ti_3SiC_2 of reference samples were measured using a PHI 5700/660 Physical Electronics Photoelectron Spectrometer at the University of Silesia, Poland. The hemi-spherical mirror analyser provided the energy of the electrons with resolution of about 0.3 eV. The surface charging was controlled at the adventitious C 1s line and the energy scale was normalized to the value of binding energy 284.2 eV for this line. The spectrometer was calibrated using the Ag $3d_{5/2}$ line set at the energy 368.3 eV.

3. Results

3.1 C-BN base composite

The measured XANES spectra at the K-edges of B, N and Si from a BN composite and reference samples are presented in Fig. 1. The complementary investigations of the Ti K-edge have been published elsewhere [5]. The spectra were normalized to the same intensity below the edge using linear function for pre-edge background subtraction, and above the edge by fitting the atomic background. By using XANES one can obtain chemical information about the sample in a nondestructive manner which is rather difficult to obtain by other methods [1, 2]. The edge position and the shape of a spectra are sensitive to valence state of a probed element and coordination environment. Therefore, XANES can be used as a fingerprint to identify phases. XANES spectrum of composite is a mixture of spectra from all compounds of given elements present in the composite. The spectrum of composite can be modelled by fitting of a linear combination of known spectra of reference samples. The calculation of the content and type of phase was carried out using XANDA program [8, 9]. This program is based on the Principal Component Analysis and linear combination of the

standard compounds [3]. The result of the analysis is collected in Table 1 and comparison of model with measured spectra is shown in the Fig. 2. The content of the detected phases presented in Table 1 is an average of values derived from the analysis of given elements forming this compound (e.g. in the case of BN the K-edge of B and N was analyzed separately). From the analytical point of view, it is very useful to compare the obtained content of phases with the results from other techniques. As a complementary method the XPS was used. Each element in the XPS spectrum has a unique binding energy of a particular electron orbital, and the spectral peaks from a mixture are approximately the weighted sum of the elemental peaks from the individual constituents.

In Table 1 the results of analysis of photoelectron orbital lines are shown. The photoelectron spectra of the B 1s, Si 2p, N 1s, Ti $2p_{3/2}$ and C 1s from composite were measured. The raw data were analysed by Origin 7.0 software. The straight-line background subtraction was applied to all spectra. Then peaks were fitted with Gaussian shape function to deconvolute overlapping peaks located at the energy position characteristic for the orbital bond of a given compound. The orbital position was stated according to the literature assignment for studied phases [10- 18] and for ternary compounds according to the energy position estimated from measured spectra. For each compound, appropriate orbital lines of all elements were analysed and peak area values were taken in the stoichiometric proportion. This procedure remarkably limited the amount of possible fitting parameters. The values collected in Table 1 are the average values taken from the analysis of each element orbital (e.g. for BN one estimation resulted from analysis of 1s B orbital and second from analysis of 1s orbital of N. In a case of ternary compound three orbitals were analysed). The error indicated for XANES and XPS results is the difference between the value of phase determined from each element orbital in the compound and the average value. The error indicated for XANES and XPS results is the difference between the value of phase estimated

from each element spectra in the compound and the average value. The total concentration of existing compounds was taken as 100 percent. The comparison of measured spectra for considered orbitals and the best fit used for the quantitative phase analysis of composite is presented in Fig. 3. It is important to notice that the mean free path of photoelectrons measured by XPS is very small. The electrons which are detected in this experiment originate from 1 - 5 nm region below the sample surface.

3.2 Ge low-dimensional structures

The normalized oscillations $\chi(k)$ of EXAFS spectra for investigated and standard samples are shown in Fig. 4. It was shown earlier [7] that the 'characteristic minimum' in the region of about 4 Å^{-1} (corresponding to that in pure crystalline Ge) transforms in Ge$_x$Si$_{1-x}$ into an oscillation maximum for samples with a high content of Si atoms surrounding the Ge central atom. This maximum arises from the increasing contribution of the Si backscattering amplitude which differs considerably from the Ge one. This feature has been interpreted in reference [19] as the fingerprint of the presence of Si atoms around Ge. For x = 50% this maximum is already very pronounced.

From the qualitative analysis of EXAFS oscillations it can be noticed that the local structure around Ge atoms in investigated samples is similar to the one in Ge$_x$Si$_{1-x}$ alloys with content of Si atoms smaller than $x = 0.5$.

To gain more quantitative information the first coordination shell was fitted for all samples assuming both Ge-Ge and Ge-Si correlations. As it was mentioned above we assumed that the local microstructure around Ge atoms can be considered as an alloy of germanium and silicon, where the number x of the Ge atoms located as the nearest neighbors around the central atom is smaller than that in pure Ge (N=4). To model the situation inside the investigated structures we assumed presence of the pure Ge where some Ge atoms were replaced by Si atoms, as a result of intermixing at the Ge/Si interfaces. The coordination

numbers around Ge absorbing atom are $N{\cdot}x$ for Ge atoms and $N{\cdot}(1\text{-}x)$ for Si atoms. The amplitude and phase calculations were done with the averaged orientation of polarization vector relative to crystallographic axis and coordination number equal to 4 for all samples.

In Fig. 5 the magnitude of the Fourier transform of the Ge EXAFS is presented for investigated samples. One can see that the first coordination shell shifts to the lower R (in the case of 7ML sample this shift is more significant). It can be related to both, presence of Si atoms in the first coordination shell and stress in Ge layer originated from the substrate and capped layer.

In Figs. (6 a, b) the fitting of the Fourier back transformation (FBT) of the first coordination shell is shown. The limits of R for FBT were 1.60 – 2.57 Å and 1.61 – 2.55 Å for 7 ML and 12 ML samples, respectively. One can see a good agreement between the model and experimental data. In Table 2 the numerical results of fitting procedure are collected. The indicated errors in the determination of the fitting parameters were evaluated by the Artemis program.

From HREM images of the sample with nominal 7ML of Ge (Fig. 7) one can see that contrast along the layer is changing. There are some areas that appear darker than the others. This might suggest a non-uniform distribution of Ge. Taking into account the thickness of a layer with a dark contrast would suggest that the thickness of the Ge layer is 1.7nm. This layer is covered by a 17nm Si capping layer of high crystallographic perfection.

The sample with nominal 12ML of Ge has 2.5nm thick Ge layer covered by 17.5nm Si capping layer (Fig. 8). Ge quantum dots are clearly seen in this sample. Formation of planar defects in the Si capping layer can be noticed. They originate from the Ge layer (marked by arrows in Fig. 8). The planar defects are also visible in low magnification images obtained under two beam conditions with g-vector $\underline{1}1\underline{1}$ (Fig. 9b) and $02\underline{2}$ (Fig. 9c). These defects are stacking faults formed on {111} planes of Si.

4. Discussion

4.1 C-BN base composite

As mentioned in the previous chapter XANES and XPS provide information from different regions of the sample. The information in the XANES comes from a depth ~ 20 nm whereas in the XPS technique signals are registered from the surface ~5 nm only. This allows us to learn about the spatial distribution of particular phases in the BN-base composite. Comparing the XPS and the XANES results suggests an inhomogeneous distribution of constituent phases in the studied sample. The composite consists of c-BN grains surrounded by compositionally different phases [5]. The fact that the c-BN is seen by XPS at the level of 11% indicates that only this fraction of c-BN grains is close to the sample surface and it is not covered by other constituent phases. Based on the preparation procedure we know that the concentration of $TiSi_2$ and Si_3N_4 compounds is small in the composite. The fact that these two phases are seen by XPS suggests their location is at the top of the BN grains. The content of these phases in the near surface region exceeds 60 % of that of bulk. In contrast, the content of the $TiC_{0.3}N_{0.7}$ phase is almost twice higher in the bulk compared to the surface. We conclude that this phase is located close to the c-BN grains deeper in the sample. The TiB_2, TiC and SiC compounds are roughly homogeneously distributed in the whole volume of BN-base composite. The SiO_2 compound was also detected using XPS analysis. The amount of this compound doesn't exceed 5 %. Since XPS technique is surface sensitive, the existence of a SiO_2 phase can be explained by attraction of oxygen from atmosphere by Si atoms located close to the surface.

4.2 Ge low-dimensional structures

Fitted fraction of Ge in 7ML and in 12ML sample is equal to ~72±3 % and to 85±1.5%, respectively. Therefore, it is reasonable to compare our fitting parameters to those

reported for $Ge_{0.74}Si_{0.26}$ and $Ge_{0.82}Si_{0.18}$ alloys [20, 21] with the Si concentration closest to that found in the investigated structures. The Ge-Ge bond length for 7ML and 12 ML structure is shorter by 0.02 Å in comparison with Ge-Ge bond length for $Ge_{0.74}Si_{0.26}$ and $Ge_{0.82}Si_{0.18}$ alloys. This might indicate the presence of compressive strain on these bonds. On the other hand the Ge-Si bond lengths and the numbers of Ge and Si atoms in the first coordination shell are the same within the limits of calculated errors as these observed in above mentioned composite. This also might suggest the existence of two regions inside the Ge QDs, the Ge core and intermixed surface region. If one estimates the thickness of the "intermixed region", assuming Si atoms situated only at the interfaces (between the quantum dot core and the surface layer surrounding this core), following the approach suggested in [23], then the thickness of the "intermixed region" for the samples with the nominal 7 and 12 ML of Ge is 1 to 2ML.

Moreover, comparing the Debye-Waller[1] (DW) factor for Ge-Si alloys and our investigated quantum dots one can notice the reduction of DW factor for Ge-Ge correlations from 0.0047 (for an alloy $Ge_{0.74}Si_{0.26}$) to 0.002 $Å^2$ (for 7 ML sample). Some difference could be explained by the difference in the measurement temperature[1]. The 7ML sample was measured at the liquid nitrogen temperature and the $Ge_{0.74}Si_{0.26}$ alloy was measured at the room temperature. For the 12 ML sample and $Ge_{0.82}Si_{0.18}$ alloy the DW factor is in the same order of magnitude and both samples were measured at room temperature. Nevertheless, the pronounced increasing of DW factor for Ge-Si correlations for both samples can be observed, which cannot be related to thermal disorder. Thus it should be related to the chemical disorder in the Ge-Si correlations in the investigated Ge-quantum dots samples, confirming the existence of the pure Ge core and a disordered surface layer with Si atoms situated only at the interfaces. In addition to foregoing description we can also estimate the contribution of Si atoms located at the surface based on simple geometrical model and knowing the average size (height and base) of QDs from the TEM images and assuming the presence of pure Ge in the core of QDs. In the case of 12ML sample an 11% contribution of Si atoms from the surface

---

[1] Decreasing of the measurement temperature causes reduction of the full DW factor in view of decreasing of its thermal term: $\sigma^2_{full} = \sigma^2_{therm} + \sigma^2_{stat}$.

has been found. The EXAFS analysis provided the value of 15%. The difference between geometrical model and EXAFS value is about 4% and this can be related to the dispersion of the QDs size and diffusion of some Si atoms inside the second layer of the formed QDs. We cannot carry out a similar analysis for the sample with nominal 7 ML of Ge since we do not observe formation of QDs by TEM.

Lets consider now, the compressive strain and kind of defects observed by TEM. These studies confirm the presence of compressive strain in iSi/Ge/Si structures. It was shown earlier that for some critical layer thickness of Ge (about 11-12 ML) a partial relaxation of elastic strain in Ge layer could occur [22]. Therefore, if this critical thickness of Ge is exceeded misfit dislocations and stacking faults (with partial dislocations at their ends) are formed and propagate to the sample surface. For a layer with a larger thickness of Ge the density of dislocations at the interfaces and inside the formed low-dimensional structures is increasing. Therefore, a number of the stacking faults in Si capping layer also becomes larger, since dislocations need to propagate to the sample surface.

Planar defects in the capping layer, similar to these observed in the sample with 12ML, were visible in the high resolution images of the sample with 20ML thickness of Ge layer (not shown here). These defects originate at the base of the quantum dots and propagate through the Ge layer and a capping Si layer to the sample surface. The density of the defects is higher than for 12ML sample. This indicated that 12ML sample is only partially relaxed. It was observed that creation of dislocations degraded the optical properties of the investigated structures.

5. Conclusions

In the presented paper two approaches to determine the composition of constituent phases from disordered materials have been used: the linear combination of the XANES

spectra of the reference compounds and the deconvolution of the XPS spectra. We took advantage of both methods by performing spectral identification and quantification of Si, B, N, C and Ti species and then refining the result to the compositional distributions in the studied sample. XANES analysis based on the linear combination of standard spectra proved to be a useful tool to answer the question how many and what kind of phases were formed during technological process of BN-composite preparation. The comparison of XANES and XPS analysis provided additional information about space distribution of phases around c-BN grains.

EXAFS studies of the local Ge-atom envinroment, in Ge quantum dots imbedded in Si ,matrix, showed that Ge-Ge bond lengths are shorter than the bond lengths in pure Ge, $Ge_{0.74}Si_{0.26}$ or $Ge_{0.82}Si_{0.18}$ alloys. This suggests that the Ge-Ge bonds in the investigated QD structures are under compressive strain. The magnitude of DW factor indicated a large disorder of Si atoms, thus suggesting that Si atoms, are located only or close to the surface of QDs. The thickness of the "intermixed region" rich in Si in the investigated samples was about 1-2ML. Consideration of a geometrical model with a QD size obtained from TEM measurements found a concentration of Si atoms close to that obtained from the EXAFS analysis, thus confirming that Si atoms are present only at the surface of the monocrystal Ge core of QD.

Based on two examples of two different materials we demonstrated the usefulness of x-ray absorption spectroscopy to obtain quantitative information on the atomic level.

References

[1] D. C. Koingsberger, R. Prins, X- ray Absorption: Principles, Application, Techniques, John Wiley, New York (1988).

[2] J. Kawai, Absorption Techniques in X- rays Spectrometry, Encyclopedia of Analytical Chemistry, R. A. Meyers (Ed.), pp 13288- 13315, John Wiley & Sons Ltd, Chichester, 2000.

[3] S. R. Wasserman, J. Phys. IV, 7, C2- 203- 5 (1997).

[4] E. Benko, J. Skrzypek, B. Królicka, A. Wyczesany, T.L.Barr, Diamond and Related Materials 8, 1838- 46 (1999).

[5] E. Piskorska, K. Lawniczak-Jablonska, I.N. Demchenko, R. Minikayev, E. Benko, P. Klimczyk, A.Witkowska, E. Welter, M. Heinonen, J. of Alloys and Compounds, <u>382</u> (2004) 187.

[6] I.N. Demchenko, K. Lawniczak-Jablonska, K.S. Zhuravlev, E.Piskorska, A.I. Nikiforov, E. Welter, *Acta Phys. Polonica A,* 101, 709, 2002.

[7] I.N. Demchenko, K. Lawniczak-Jablonska, E. Piskorska, K.S. Zhuravlev, A.I. Nikiforov, E. Welter, *J. Alloys and Comp.*, 382, 206, 2004.

[8] K. V. Klementiev, XANES dactyloscope for Windows, K.V. Klementiev, XANES dactyloscope for Windows, freeware: www.desy.de/~klmn/xanda.html

[9] K. V. Klementiev, J. Phys. D: Appl. Phys. 34 (2001) 209- 217.

[10] A. A. Galuska, J. C. Uht, N. J. Marquez, Vac. Sci. Technol. A6, (1988) 110- 22.

[12] L. Ramqvist, K. Hamrin, G. Johansson, A. Fahlman, C. Nordling , J. Phys. Chem. Solids, Vol 30, (1969) 1835- 47.

[13] G. Mavel, J. Escard, P. Costa, J. Castaing, Surf. Sci. 35, (1973) 109- 16.

[14] A. A. Galuska, J. C. Uht, N. J. Marquez, Vac. Sci. Technol. A6, (1988) 110- 22.

[15] H. Ihara, Y. Kumashiro, A. Itoh, K. Maeda, Jpn. J. Appl. Phys. 12, (1973) 1462- 3.

[16] R. Bertoncello, A. Casagrande, M. Casarin, A. Glisenti, E. Lanzoni, L. Mirenghi, E. Tondello, Surface And Interface Analysis, Vol 18, (1992), 525- 31.

[17] V.I. Nefedov, D. Gati, B. F. Dzhurinskii, N. P. Sergushin, Y. V. Salyn, Zh. Neorg, Khimii, 20 (1976) 551- 8.

[18] M. Cardona and L. Ley, Eds., Photoemission in Solids I: General Principles (Springer-Verlag, Berlin, Introduction (to 'Photoemission in solids'), (1978) 1- 104.

[19] F. d'Acapito, P. Castrucci, N. Pinto, R. Gunnella, M. De Crescenzi, I. Davoli, *Surface Science* 518, 183, 2002.

[20] H. Kajiyama, S. Muramatsu, T. Shimada et al., *Phys. Rev. B*, 45, 14005, 1992.

[21] D.B. Aldrich, R.J. Nemanich, D.E. Sayers, *Phys. Rev. B*, 50, 15026, 1994.

[22] I.N. Demchenko, *PhD thesis*, Institute of Physics PAS, 2005.

[23] Y.L. Soo, G. Kioseoglou, S. Huang, S. Kim, Y.H. Kao, Appl. Phys. Lett., 78, 3684, 2001.

Figure captions

Fig. 1.

XANES of spectra for composites $BN+Ti_3SiC_2$ and for the reference compounds:

a) B K-edge; b); Si K-edge c) N K-edge.

Fig. 2.

XANES of spectra and their fit with the spectra of the reference compounds for composite: a)

B K-edge; b) Si K-edge; c) N K-edge.

Fig. 3.

The fitting procedure and possible peak identifications for XPS elements lines for the

composite.

Fig. 4

Weighted EXAFS oscillations $\chi(k)$ for the samples (top-down): Ge - powder,

Si/7ML Ge/Si(001), Si/12ML Ge/Si(001), $Ge_{0.5}Si_{0.5}$/Si(001).

Fig. 5.

Experimental radial distribution function of atoms around Ge for the samples (top-

down): Ge – powder; Si/7ML Ge/Si(001); Si/12ML Ge/Si(001).

Fig. 6 a,b).

Least-squares fitting of the first coordination shell EXAFS oscillations (dot grey line) and

the experimental data (thin line) for: a) Si/7ML Ge/Si(001); b) Si/12ML Ge/Si(001)

samples.

Fig. 7.

Cross-section HREM image of the nominal 7ML of Ge layer grown on the Si(001)

substrate.

Fig. 8.

Cross-section HREM image of the nominal 12ML of Ge layer grown on the Si(001) substrate. Note stacking faults (indicated by black arrows) formed in a Si cap layer.

Fig. 9.

Two-beam bright-field images (low magnification) of the sample with the nominal 12 Ml of Ge grown on Si substratesi shown in three different diffraction conditions:

a) with g-vector $\underline{4}00$;

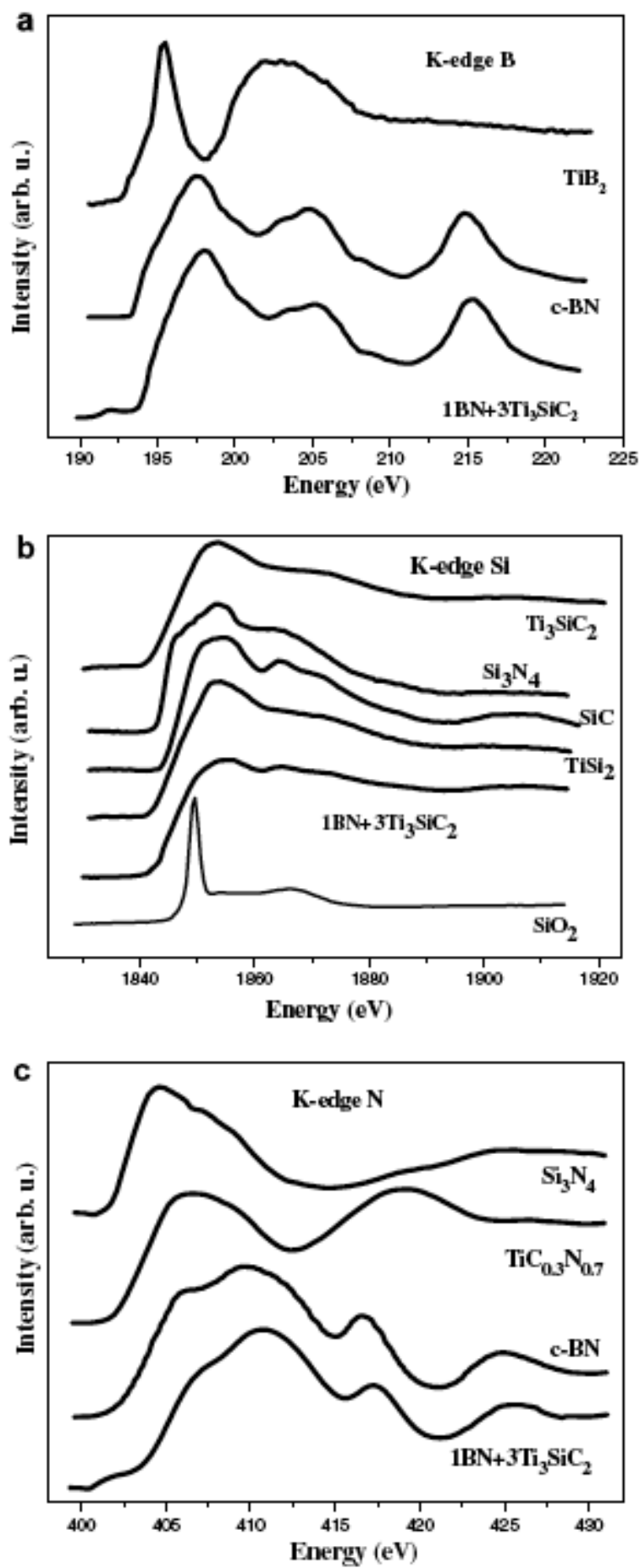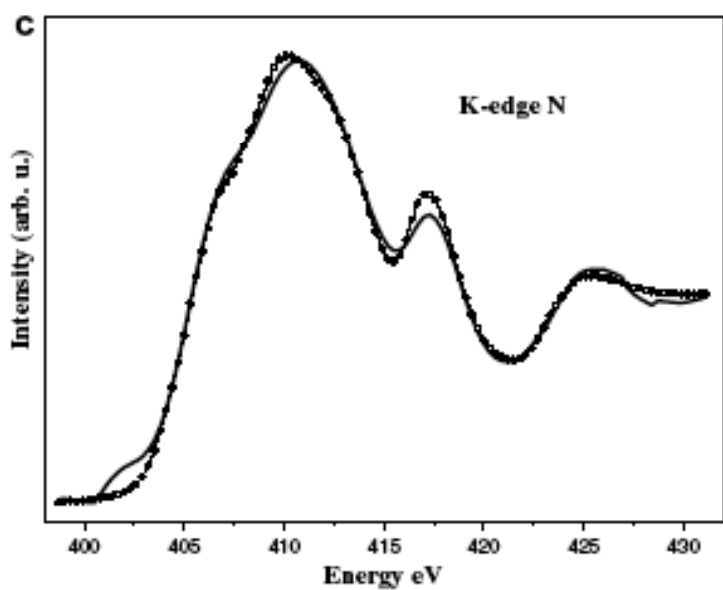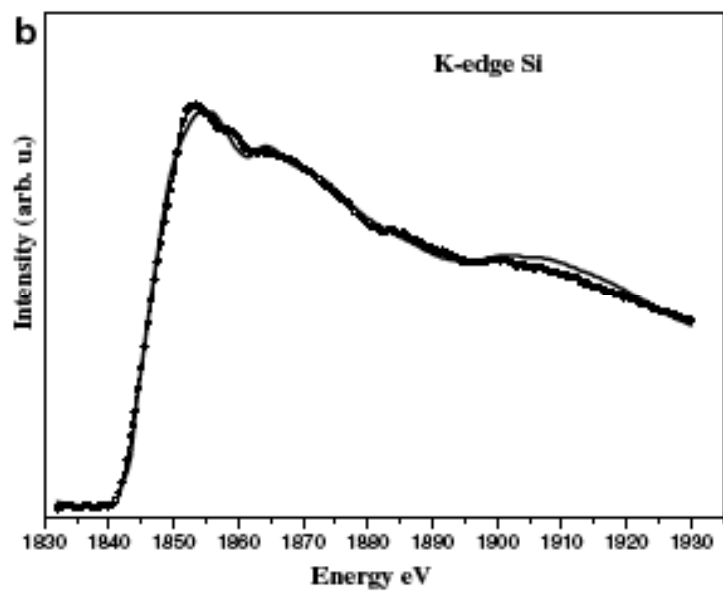b) with g-vector $\underline{1}1\underline{1}$;

c) with g-vector $02\underline{2}$.

Fig. 1

a

Intensity (arb. u.)

K-edge B

1BN+3Ti₃SiC₂

fit

Energy eV

b

Intensity (arb. u.)
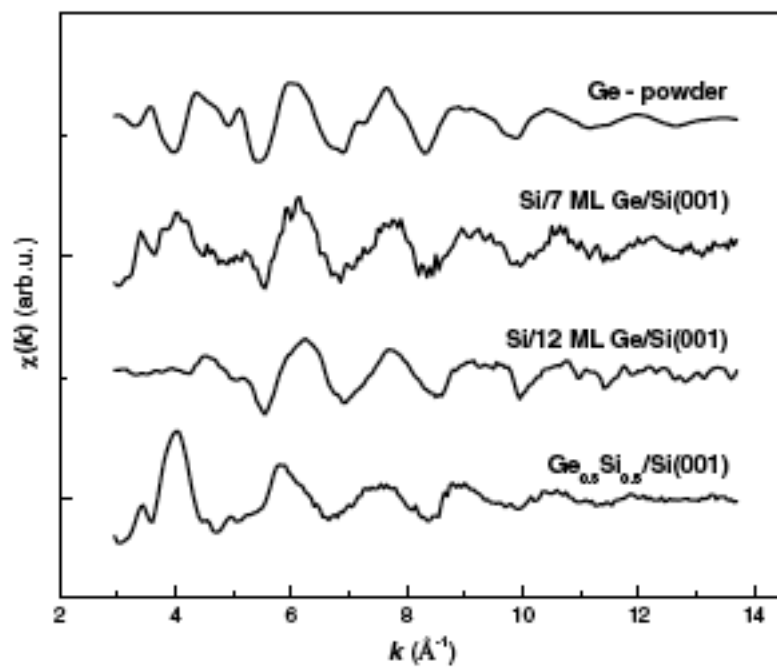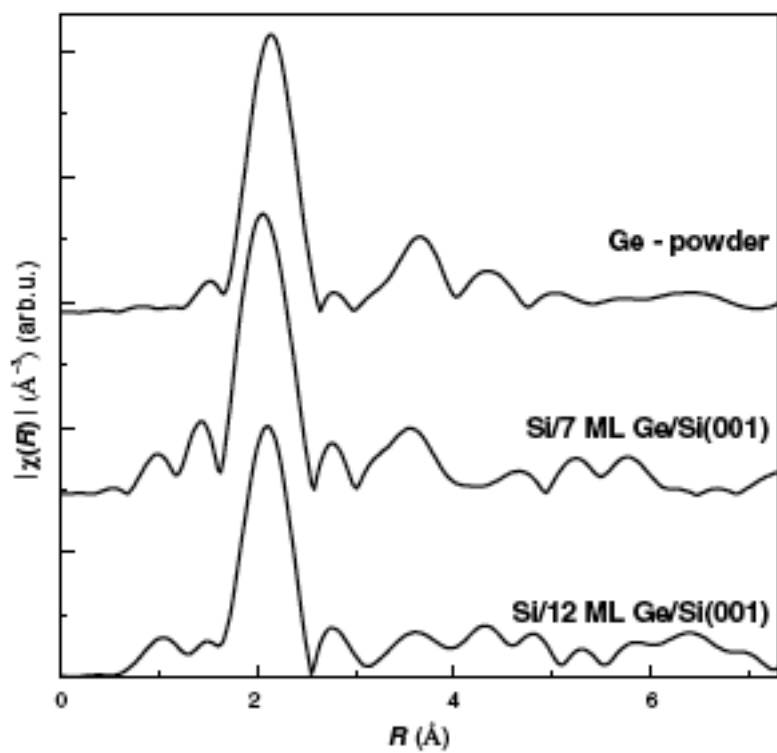
K-edge Si

Energy eV

c

Intensity (arb. u.)

K-edge N
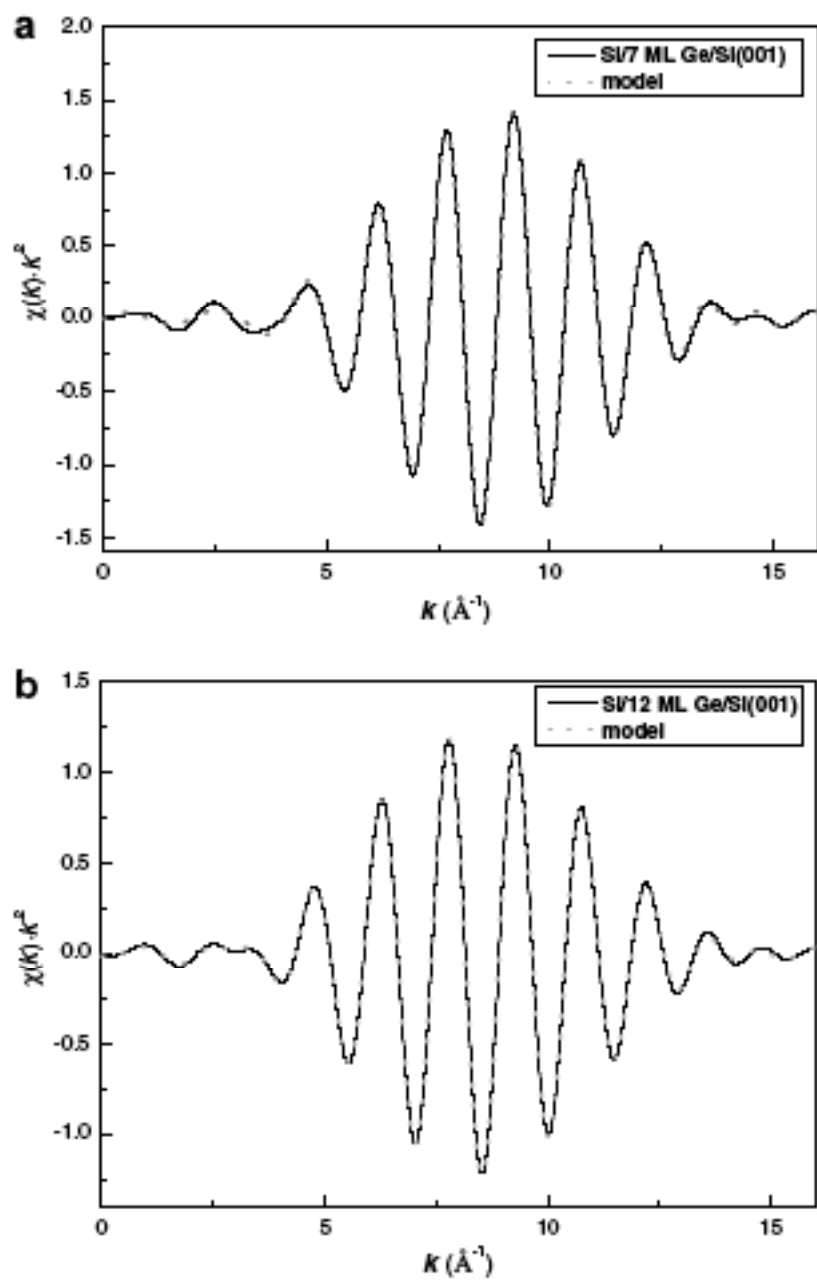
Energy eV
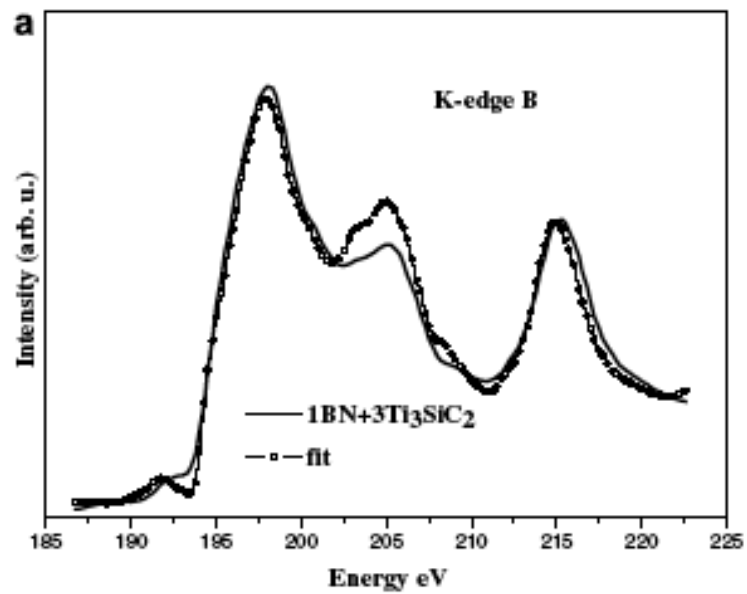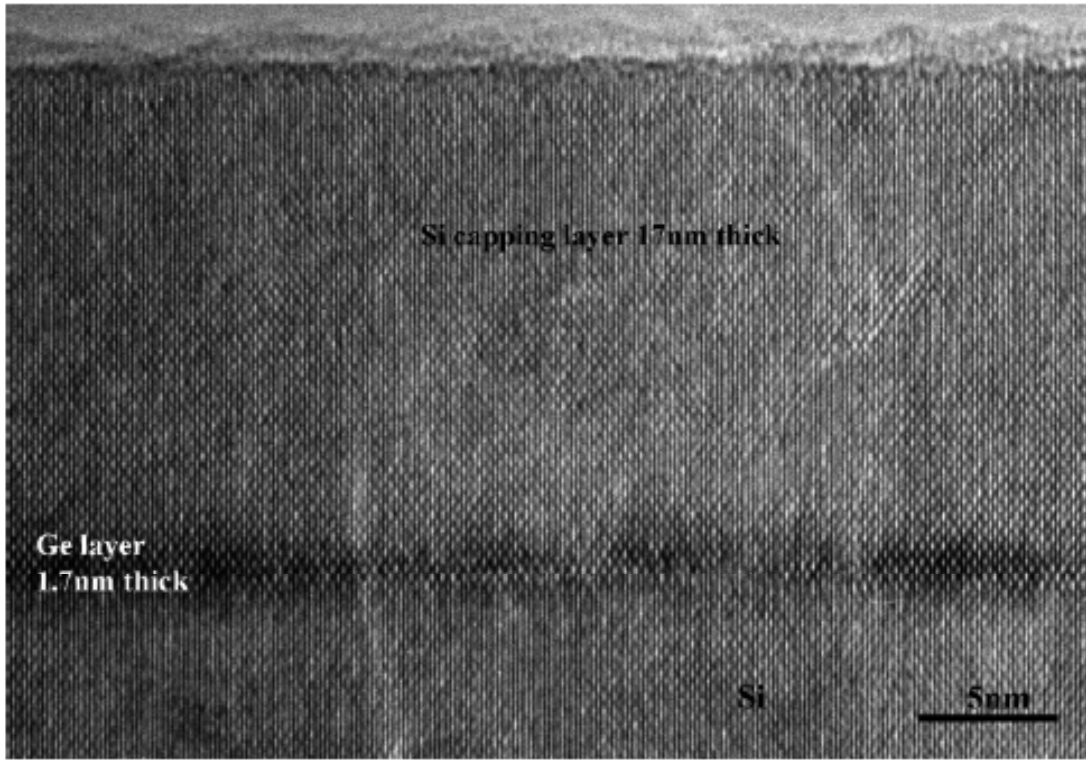
Fig. 2

Fig. 3.

Fig. 4.

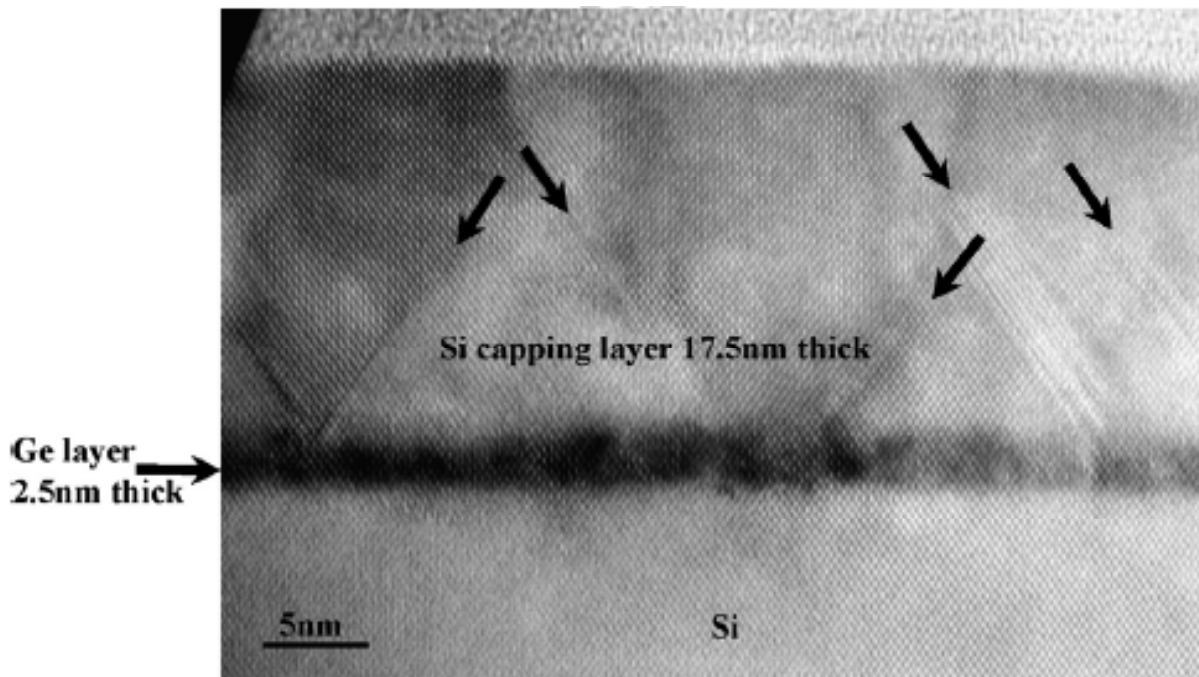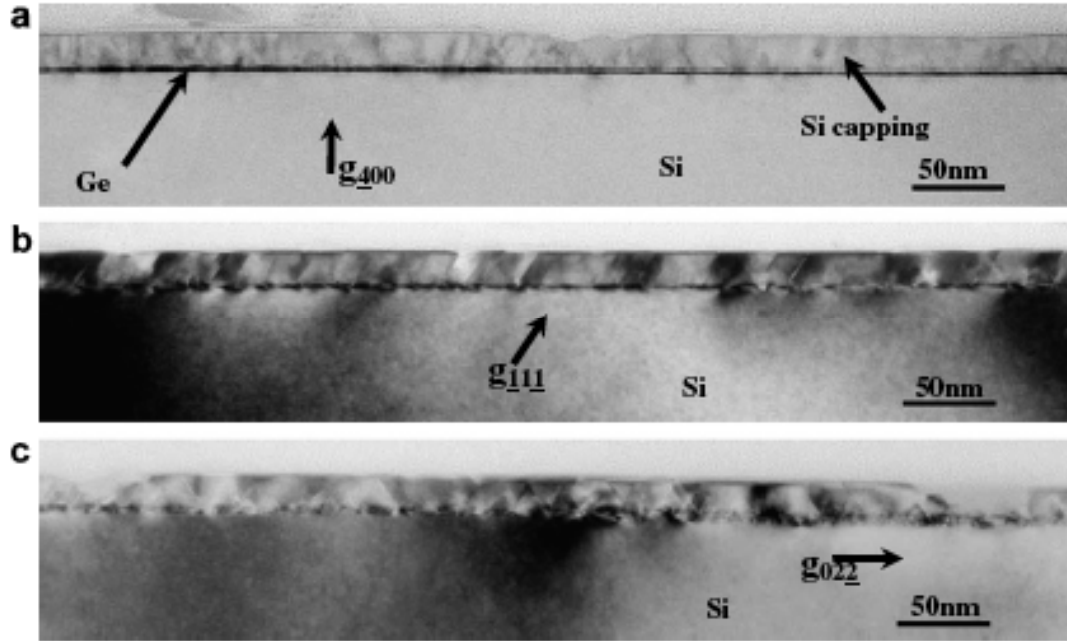Fig. 5.

22
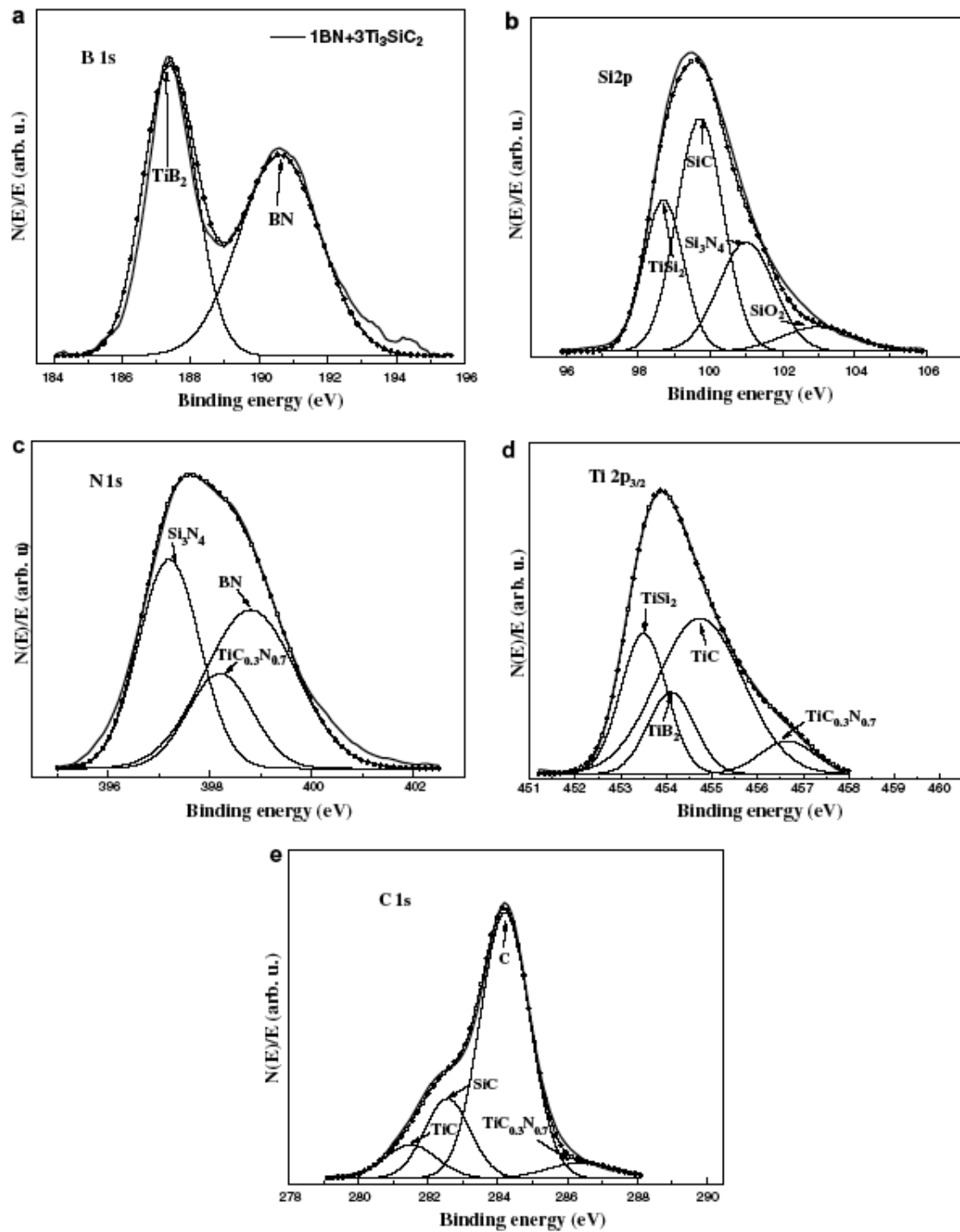
Fig. 6.

Fig. 7.

Fig. 8.

Fig. 9.

Table 1
Compounds found in c-BN composites and their percentage shares contents estimated by XANES and XPS analysis

Compound	XANES	XPS
TiB_2	11 ± 1	7 ± 3
c-BN	28 ± 4	11 ± 1
$TiSi_2$	2 ± 1	10 ± 3
TiC	12 ± 1	17 ± 3
$TiC_{0.3}N_{0.7}$	12 ± 1	4 ± 1
SiC	30 ± 1	33 ± 3
Si_3N_4	5 ± 1	13 ± 6
SiO_2	–	5 ± 1

Table 2
Bond lengths, R, coordination numbers, N, and Debye–Waller factors for investigated and reference samples from EXAFS analysis

Sample	Bonds	R (Å)	N	σ^2 (Å^2)	R-factor of fit	Reference
7 ML, $T_g^{Ge} \sim 210\,°C$	Ge–Si	2.41 ± 0.04	1.12 ± 0.12	0.011 ± 0.004	0.003	This work
	Ge–Ge	2.420 ± 0.002	2.88 ± 0.12	0.0020 ± 0.0002		
$Ge_{0.74}Si_{0.26}/Si(001)$	Ge–Si	2.400 ± 0.018	1.2 ± 0.2	0.0044	–	[19]
	Ge–Ge	2.439 ± 0.005	3.2 ± 0.3	0.0047		
12 ML, $T_g^{Ge} \sim 210\,°C$	Ge–Si	2.40 ± 0.03	0.59 ± 0.06	0.011 ± 0.003	0.001	[7]
	Ge–Ge	2.418 ± 0.001	3.41 ± 0.06	0.0041 ± 0.0001		
$Ge_{0.82}Si_{0.18}/Si(001)$	Ge–Si	2.394 ± 0.04	0.8 ± 0.2	0.00452	–	[20]
	Ge–Ge	2.442 ± 0.009	3.2 ± 0.7	0.00457		